15th Triennial World Congress, Barcelona, Spain

DESIGN AND CONTROL OF A NOVEL PLANAR MAGLEV POSITIONING SYSTEM

Mei-Yung Chen[*], Ming-Chiuan Shiu[*], Tzuo-Bo Lin[*], Li-Chen Fu[*,]**

** Department of Electrical Engineering, National Taiwan University, Taipei, Taiwan, Republic of China.*
*** Department of Computer Science and Information Engineering, National Taiwan University, Taipei, Taiwan, Republic of China.*

Abstract: This paper describes a novel planar repulsive maglev prototype. In this maglev system, the carrier is levitated by a planar 2D array of coils. The levitation forces are due to repelling between the magnets and the coils. Then, the general model of motion of the carrier with complete degree of freedoms(DOFs) is derived and analyzed. Next, for the sake of control, a PID controller is designed here to regulate the all DOFs of the planar maglev system. From the simulation results, satisfactory good performances including stiffness and precision have been demonstrated. The experiment of the proposed system is under preparation. *Copyright ©2002 IFAC*

Keywords: Magnetic suspension, Modelling, Regulation, Positioning system, PID controller

1. INTRODUCTION

In the real world, besides air bearings, free-floating levitation can be achieved by two methods: one with electrostatic levitation and the other with magnetic levitation (abbreviated as maglev). In the former, electrostatic charges of the same or the opposite polarity are deposited on two opposing objects. Levitation is achieved by the attractive force due to the opposite polarity or by repulsive force due to charges of the identical polarity. In the latter maglev system, attractive as well as repulsive levitation can be obtained in the same fashion.

Recently, magnetic levitation is considered as one of the most suitable ways to achieve the high precision transportation. From the previous research results, some just discussed a single-axis maglev system (Wang and Ilene, 1993; Chen, et al., 2000), but some others (Kim, et al., 1997; Chen, et al., 1999) have expanded the single-axis system into a dual-axis double-decked or planar system. However, in the literature there are relatively fewer works which investigate the planer dual-axis maglev positioning system. In this paper, we build a novel planar maglev platform to achieve the objective of 2D high-precision positioning. A new mathematical model is first derived, based on which a PID controller is then designed to achieve satisfactory system performance. To demonstrate the effectiveness of the entire system design, simulation results are provided for verification.

In this paper, design, analysis and control of a novel planar maglev positioning system is presented. Several salient features of the current research work include: (1) successful development of analytical tools for predicting electromagnetic properties: field solutions can be easily desired using magnetic flux density and vector potential, (2) both electromagnetic and mechanical design for a maglev platform, and (3) theoretical validation through extensive numerical

simulation subject to a PID controller for achieving six-DOFs regulation.

2.MAGLEV SYSTEM DESIGN CONCEPT

In this section, some basic concepts about physics and electromagnetics are important for the design of the aforementioned maglev platform. To complete the overall system design, some mechanisms have to be evaluated before we can finalize the construction components of the entire system. The overall system configuration mainly consists of two parts, namely, a carrier embedded with a number of magnets, and a bottom plate decked with a 2D matrix array of cylindrical solenoids.

2.1 Electromagnetic field -- Cylindrical Solenoid Design

In the numerical analysis, when the levitation distance between the magnet to be levitated and the cylindrical solenoid underneath is very small, the magnetic flux in between approach a constant value. The arrangement of the cylindrical solenoids and their floating currents such that a rather uniform magnetic field over a planar surface slightly above the coil array, as shown in Fig. 1. Therefore, it seems that this structure with a permanent magnet becomes the most optimal choice to meet our special purpose. Under some thorough analysis, the specifications of the cylindrical solenoids are determined such that the resistance is 2.8Ω, the thickness of wire is $0.361mm$, the inductance is $325Ts$, the number of turns is 380, and the vertical height is $10mm$.

As has been mentioned earlier, if the magnetic dipole sits on a horizontal place at a ting distance from the solenoid array then the subjected (vertical)levitation force is approximately constant over the entire plane. Thus, the force function can be desired from a simpler case with only single solenoid and a magnetic dipole over it, i.e., (Brzezina and Langerholc, 1974).

$$F_Z = \frac{m_0 (NI_z)^2 r}{2a^2}(1+\frac{a}{p\ r}), \qquad (1)$$

where m_0 = air-magnetite coefficient (permeability)
N = the number of turns of the electric wire
I_Z = current of electric wire
r = width of magnet
a = air gap of levitated object and solenoid

2.2 Carrier Design

From our forgoing research, NdFeB seems to be the best choice at present for the magnet material, because it has high coercivity and remanence. These characteristics of NdFeB magnet can produce larger

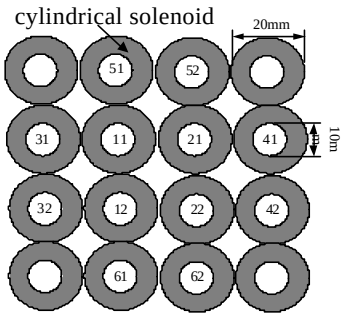

Fig. 1: The plane of the cylindrical solenoids

magnetic forces when subject to a magnetic field. Therefore, in the present work we choose such kind of magnets to be those embedded in the carrier. To keep lightweight and to avoid magnetization, the carrier is made by the material of Aluminium. In order to meet the requirement of obtaining a planar two-dimensional positioning platform, the carrier is embedded with eight stabilizing permanent magnets on the aslant sides to provide the lateral forces and with four levitating permanent magnets on the bottom of the carrier to counteract the weight of the carrier.

In the positioning system, existence of levitating force due to repelling usually causes destabilization in the lateral direction. Therefore, we design the stabilizing magnets affixed to the sides of the carrier in order to provide sufficient control force in the lateral direction. To serve this control purpose, the paired stabilizing magnets on each side are much better than a single one, since the former case can provide twice of the stabilizing force to the carrier than the latter case, and the arrangement of the aforementioned magnets is shown in Fig. 2. For a free-floating system, the total six DOFs of the carrier should be taken into consideration, namely, X, Y, Z, f, q and y where their definitions are shown in Fig.3.

2.3 System Modelling

In order to achieve the high-precision positioning performance, we must control the translation and the attitude of the carrier properly. To fulfil this purpose, a complete analytical model which includes two lateral DOFs, one propulsion DOF, and three orientational DOFs will be first derived. Before we proceed with the modeling, several technical assumptions must be made to let the task be more tractable.

Assumptions:

A. Each magnet is considered as one single dipole carrying the same magnetic dipole moment and is located at the center of each magnet.

B. The geometric arrangement of the array of cylindrical solenoids and the adjustment of their floating currents are such that there exists a plane above the top face of the array of solenoids with uniform magnetic field.

C. Any pair of permanent magnets on any side of the carrier are far separated so that the influence in between can be neglected.

Translation part; Consider the carrier to be represented by a uniform rigid-box shaped object with the center of mass coincident with the center of geometry. In the following context, we will assume that the carrier in Fig.2 suspends over the coils in Fig.1, in a way that the magnet with a label will be roughly sight on the coil with the same label. The principle of linear momentum leads to the force equation:

$$A\sum_{i=1}^{6} F_i = m\ddot{R}_G\,, \tag{2}$$

where A is the transformation matrix from the body-fixed coordinate to an inertial coordinate, m is the weight of the carrier, and R_G is the position of mass center. According to Fig. 3, Eq. (2) can be expressed as follows:

$$A\sum_{i=1}^{6} F_i = A\begin{bmatrix} F_{S3}+F_{S4} \\ F_{S5}+F_{S6} \\ F_{L1}+F_{L2}+F_{L3}+F_{L4}+F_{L5}+F_{L6} \end{bmatrix} - \begin{bmatrix} 0 \\ 0 \\ mg \end{bmatrix} = m\begin{bmatrix} \ddot{x}_G \\ \ddot{y}_G \\ \ddot{z}_G \end{bmatrix}, \tag{3}$$

where in the subscripts of the above notations the numerals correspond to the magnet labels, and *S*, *L* are to classify the interaction force into stabilization kind and levitation kind, respectively.

Rotation part; The principle of angular momentum leads to torque equations for the rotational coordinates. Form Euler's equations (Hang, 1992), the rotational dynamics with respect to the carrier body coordinate are as follows:

$$M_G = AIa + Aw \times Iw\,, \tag{4}$$

where I is the moment of inertia of the carrier in the body coordinate, and w, a are the angular velocity and acceleration also expressed in the body coordinate, respectively. As a result, the angular acceleration can be obtained as:

$$\begin{aligned} I\,a &= A^{-1}(M_G - Aw \times Iw) \\ &= \sum_{i=1}^{12} r_i \times F_i - w \times Iw\,, \end{aligned} \tag{5}$$

where r_i stands for the coordinate of the embedded in the carrier and F_i respect its subjected force so:

$$\begin{aligned} \sum_{i=1}^{12} r_i \times F_i = &\begin{bmatrix} x_{11} \\ y_{11} \\ z_{11} \end{bmatrix} \times \begin{bmatrix} 0 \\ 0 \\ F_{L11} \end{bmatrix} + \begin{bmatrix} x_{12} \\ y_{12} \\ z_{12} \end{bmatrix} \times \begin{bmatrix} 0 \\ 0 \\ F_{L12} \end{bmatrix} + \ldots \\ &+ \begin{bmatrix} x_{61} \\ y_{61} \\ z_{61} \end{bmatrix} \times \begin{bmatrix} 0 \\ F_{S61} \\ F_{L61} \end{bmatrix} + \begin{bmatrix} x_{62} \\ y_{62} \\ z_{62} \end{bmatrix} \times \begin{bmatrix} 0 \\ F_{S62} \\ F_{L62} \end{bmatrix} \triangleq \begin{bmatrix} T_x \\ T_y \\ T_z \end{bmatrix}. \end{aligned} \tag{6}$$

Because the carrier is of geometrically symmetric shape, the moment of inertia I represented with respect to the body fixed coordinate will satisfy the following: $I_{xy} = I_{yx} = I_{xz} = I_{zx} = I_{yz} = I_{zy} = 0$, and hence

$$w \times Iw = \begin{bmatrix} w_x \\ w_y \\ w_z \end{bmatrix} \times \begin{bmatrix} I_{xx} & -I_{xy} & -I_{xz} \\ -I_{yx} & I_{yy} & -I_{yz} \\ -I_{zx} & -I_{zy} & I_{zz} \end{bmatrix} \begin{bmatrix} w_x \\ w_y \\ w_z \end{bmatrix} = \begin{bmatrix} (I_{yy}-I_{zz})w_y\, w_z \\ (I_{zz}-I_{xx})w_z\, w_x \\ (I_{xx}-I_{yy})w_x\, w_y \end{bmatrix}. \tag{7}$$

The angular velocity $w = [w_x, w_y, w_z]$ associated with Eulerian angles f, q and y are:

$$\begin{aligned} w_x &= \dot{y} - \dot{q}\sin f \\ w_y &= \dot{f}\cos y + \dot{q}\cos f \sin y \\ w_z &= \dot{q}\cos f \cos y - \dot{f}\sin y \end{aligned}\,. \tag{8}$$

For small angles, the angular accelerations can be approximated as follows:

$$\begin{aligned} a_x &= \dot{y} - [\ddot{q}\ddot{f} + \dot{q}\dot{f}] \\ a_y &= \ddot{f} - [\dot{f}\dot{y}\dot{y} - \ddot{q}\dot{y} + \dot{q}\dot{f}\dot{f} - \dot{q}\dot{y}] \\ a_z &= \ddot{q} - [\dot{q}\dot{f}\dot{f} + \dot{q}\dot{y}\dot{y} + \ddot{f}\dot{y} + \dot{f}\dot{y}] \end{aligned} \tag{9}$$

For small angular motions, the terms in brackets on the right hand side (RHS) of Eq.(9) are negligible compared to the major terms $\ddot{y}$, $\ddot{f}$ and $\ddot{q}$, i.e., pitch, roll and yaw accelerations. Such approximation can be validated, for example, when the magnets on the carrier are 1*cm* apart and the air gap between the magnets and top face of the solenoids is about 1*mm* corresponding to angular displacements of the order of 5 mrad. The equations describing the angular motions can therefore be approximated as follows:

$$T_x = I_{xx}\ddot{y} \qquad T_y = I_{yy}\ddot{f} \qquad T_z = I_{zz}\ddot{q} \tag{10}$$

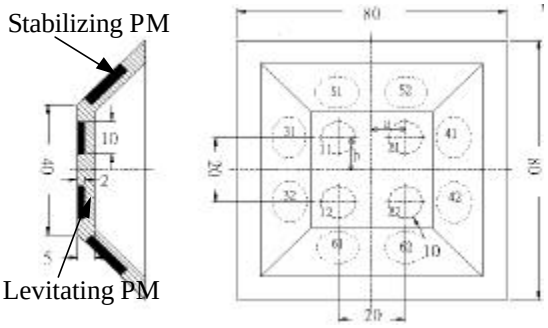

Fig. 2: Various views of the carrier

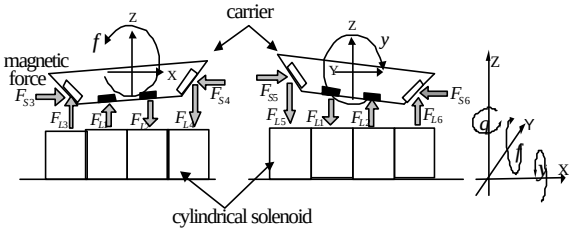

Fig. 3: Control force acting on the carrier

Based on Eqs.(3) and (10), we then are able to derive the dynamics of the carrier successfully. Then, we redefine the control inputs, currents of the solenoids underneath the carrier, as $u_1 = I_{11} = I_{12}$, $u_2 = I_{21} = I_{22}$, $u_A = I_{31} = I_{32}$, $u_B = I_{41} = I_{42}$, $u_C = I_{51} = I_{52}$, $u_D = I_{61} = I_{62}$, where the I_{ij} is the currents of the solenoid with label *ij* referring to Fig.1. Finally, the full DOFs equations of motion can be obtained as:

$$
\begin{aligned}
M\ddot{X} &= 4K_{FXL}X + 2K_{IXS}(u_A + u_B) \\
M\ddot{Y} &= 4K_{FYL}Y + 2K_{IYS}(u_C + u_D) \\
M\ddot{Z} &= 4K_{FZL}Z + 2bK_{FZS}(u_2 - u_1)f + K_{IZL}(u_A + u_B + u_C + u_D) \\
I_{zz}\ddot{q} &= 4a^2K_{FXL}q + 2aK_{IXS}(u_A + u_B + u_C + u_D) \\
I_{yy}\ddot{f} &= 2bK_{FZS}(u_2 - u_1)\ X - 2abK_{FZS}(u_1 + u_2)\,y \\
&\quad + 4b^2K_{FZL}f + bK_{IZL}[(u_A - u_B) + (u_C - u_D)] \\
I_{xx}\ddot{y} &= -2abK_{FZS}(u_1 + u_2)f + 4a^2K_{FZL}y + K_{IZL}(u_A + u_B - u_C - u_D)
\end{aligned}
\qquad (11)
$$

where I_{xx} , I_{yy} and I_{zz} represent the moment of inertia of the carrier with respect to principal *X* ,*Y* and *Z* axes, respectively, $K_{F(\ )(\ )}$ are destabilizing force constants, $K_{I(\ )(\ )}$ are constants related to the stabilizing forces and the driving currents. More detailed modelling process and parameter definitions can be found in (Shiu, 2001).

2.4 Platform

The bottom part of the platform is devised to provide levitation force to the carrier. Recalling the lateral instability due to repelling in the vertical direction, to prevent the carrier from falling damage as a result of surge movement, some safety measure is undertaken by setting up the surrounding blocking boards. The bottom part of the platform consists of a dented plate used to dock the array of cylindrical solenoids systematically, and one to more spacers need to accommodate the driver circuits, as shown in Fig.4. Obviously, the design of this positioning system can be geometrically expandable since the size of the solenoid array and the space of holding the pertaining driver circuits are variable. Finally, the four sideboards are set to enclose the entire electrical circuits and to hold cooling fans for heat radiations.

3.CONTROLLER DESIGN

Mathematically, the PID control can be expressed by:

$$U_i = P_i \cdot E_i + I_i \cdot \int E_i dt + D_i \cdot \frac{d}{dt} E_i \qquad (12)$$

where P_i, I_i and D_i are the proportional gain, integral gain, and differential gain, respectively, and E is the value of the state error.

The procedure of this method, namely, the generalized Ziegler-Nichols method (Zhuang and Atherton, 1994), is briefly described below:

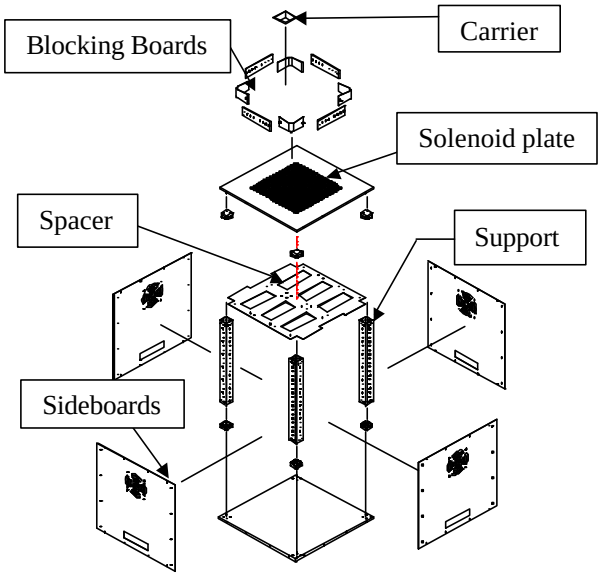

Fig. 4: The devices of the platform and assembly

(1) After linearizing the dynamic model in Eq.(11) around some operating points, we can derive an open-loop transfer function *G*(s).

(2) Choose the controlled variable weighting factors c_i (*i*=1,2,…6) for the relative control quality.

(3) Adjust the gain ($K_{P,i}$) and bring the *P*-controlled system to a stable oscillation keeping the following relationship between different loop gains G_{ii}'s as

$$\frac{K_{P,i}G_{ii}(0)}{K_{P,i+1}G_{i+1,i+1}(0)} = \frac{c_i}{c_{i+1}} \qquad i = 1,\cdots,6$$

(4) When the oscillation just commences with K_{Pj} at $K_{c,i}$, we can define the critical frequency Ω_c from the oscillation period T_c and the critical controller gain $K_{c,i}$ for the given system.

(5) From the generalized Ziegler-Nichols tuning formulas (Niederlinski, 1971), we can determine the controller parameters as listed in table 1:

Table 1: Generalized Ziegler-Nichols tuning rules

controller parameter	K_P	T_i	T_d
P	$a_1K_{c,i}$		
PI	$a_2K_{c,i}$	$0.8T_c$	
PID	$a_3K_{c,i}$	$0.5T_c$	$0.12T_c$

where $0.5 \le a_1 \le \sqrt{0.5}$, $0.45 \le a_2 \le \sqrt{0.45}$, $0.6 \le a_3 \le \sqrt{0.6}$ and the choice of the coefficients a_i depend on the ratio $a_i = \Omega_c / \nu_{i,c}$ with $\nu_{i,c}$ being the critical frequency of G_{ii}. If $a_i << 1$, a_i can be chosen at the higher value of the suggested range, and if a_i is near to one, a_i should be chosen at the lower value of the range.

(6) Check whether the relative control quality is satisfied. If not, change c_i appropriately, and then return to step 2.

From this algorithm, the PID controller gains can be determined as P={1700,1550,2000 1450,1850,1150}, I={200,200,160,80,200,40} and D={50,50,40,20,50,10}.

4. SIMULATION RESULTS

In this section, we will give some simulation results based on the mathematical model and controller we have derived so far. Some necessary system data are given as follows:

Table 2: Simulation data

Carrier Mass		$0.172kg$
Moment of Inertia	I_X	$0.000344kg.m^2$
	I_Y	$0.000344\ kg.m^2$
	I_Z	$0.0005504\ kg.m^2$
Levitating PM gap		$2mm$
Stabilizing PM gap		$3mm$
NdFeB PM dipole moment		$9.675\times10^{-8}\ A.m^2$
The distance between levitating PM and principal axes of each free body		a=b=$10mm$, c=$25mm$

Recall that the six state are X, Y, Z, q , f and y as we mentioned in section 2, and the control inputs are u_1, u_2, u_3, u_4, u_5 and u_6. First, Fig. 5 shows the time responses corresponding to the situation with the largest initial rotational error, i.e., 0.0005 rad in our mechanical system. When the carrier undergoes its largest rotational error, the corresponding transitional error should be zero in an ideal case. However, in these simulations we consider the non-ideal case here. Such non-ideal situation may result from the machining error, such as when the bottom plate which holds the cylindrical solenoids and sensors are not completely plane surface and so on. Next, Fig. 6 presents the responses due to 50g load that applied to the carrier. In that case, we can observe that all the six state signals converge to zero asymptotically as t goes to infinity. Comparing Fig. 5 and Fig. 6, respectively corresponding to empty load and 50g load, we can find difference between the two cases. When the carrier is with 50g load, the control voltages are larger than those in the case with empty load. This is rather reasonable for the performance of the PID controller that may adapt to the change of the environment to ensure the system regulating performance.

In Fig. 7, a pulse disturbance is applied to the levitated free body after the six stages converge to zero. It is found that all the states will remain to converge to the steady state, which implies that the PID controller is able to can tolerate quite large disturbance.

5. CONCLUSION

In this paper, we proposed a precision six DOFs maglev positioning system. This maglev system can be readily used in a clean room, since it will not generate wearing particle and no lubrication is required. The dynamics of the maglev system have been thoroughly analyzed and then a complete model is also derived. By this, we can understand the dynamics in detail between the levitated free body over a large number of cylindrical solenoids.

The system has been treated as a multi-input multi-output system, and a PID controller have been designed here. From the simulation results, the feasibility and effectiveness have been clearly demonstrated. And, the full experiment of the proposed system is on the way of preparation

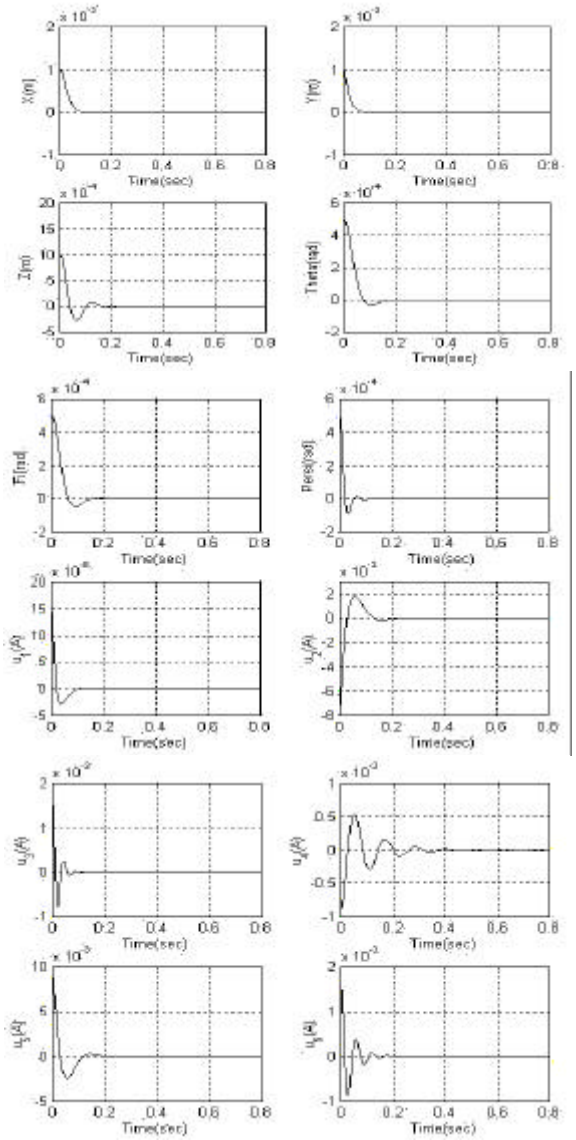

Fig. 5: The six DOFs of the carrier with maximum lateral rotation initial condition

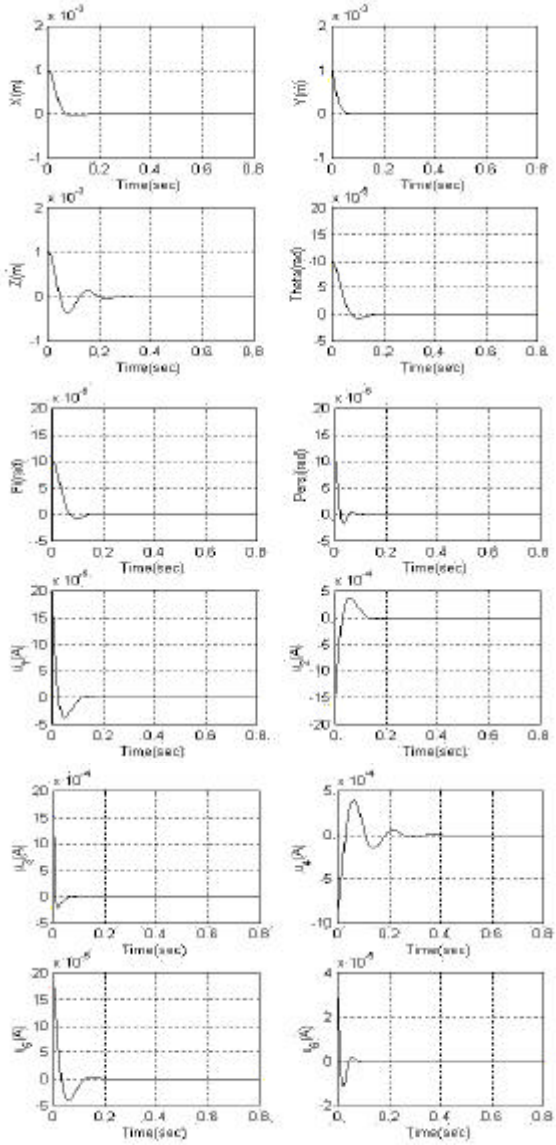

Fig. 6: The six DOFs of the carrier with 50g load

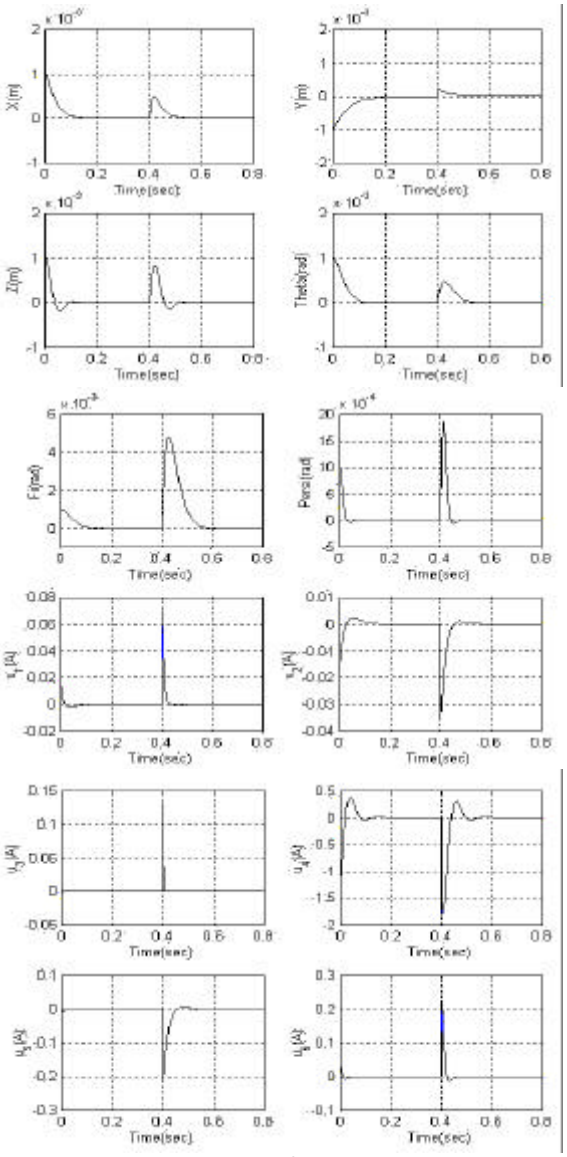

Fig. 7: The six DOFs of the carrier with pulse disturbance

REFERENCES

Wang, I.Y. and Ilene, B. V., "A New Repulsive Magnetic Levitation Approach Using Permanent Magnets and Air-Core Electromagnets" *IEEE Trans. Magnetics*, vol. 30, no. 4, July 1994, pp. 1422~1432.

Chen, M. Y., Wu, K. N. and Fu, L.C., "Design, Implementation and Self-tuning Adaptive Control of a Maglev Guiding System", *Mechatronic*, 2000, pp. 215-237

Chen, M. Y., Wang, M. J. and Fu, L.C., "Dual-Axis Maglev Guiding System Modeling and Controller Design for Wafer Transportation", *Control and Decision Conference*, 1999.

Kim, W. J., Trumper, D. L. and Long, J. H., "Modeling and Vector Control of Planar Magnetic Levitator" *IEEE Trans. Ind. Applicat.*, vol. 34, no. 6, Nov. 1998, pp. 1254~1262.

Shiu, M. C., *"Design and Control of a Novel Planar Maglev Positioning System."* Master thesis. The National Taiwan University, Taiwan, R.O.C., 2001.

Brzezina W. and Langerholc J., "Lift and side Forces on Rectangular Pole Pieces in Two Dimensions", *Journal of Applied Physics*, vol. 45, no.4, April 1974, pp.1869-1872.

Hang E.J., "Intermediate Dynamics",Prentice-Hall, 1992.

Zhuang M. and Atherton D. P., *"PID controller design for a TITO system" IEE Proc. Control Theory Appl*., vol. 141, no. 2, March 1994, pp. 111~120.

Niederlinski A., *"A heuristic approach to the design of linear multivariable interating control system." Automatica*, 1971, 7, pp. 691-701.